Journal of Hydrology 617 (2023) 129150

Contents lists available at ScienceDirect

Journal of Hydrology

journal homepage: www.elsevier.com/locate/jhydrol

Research papers

The first tree-ring reconstrruction of streamflow variability over the last ~250 years in the Lower Danube

Nagavciuc Viorica [a,b,*], Roibu Cătălin-Constantin [b], Mursa Andrei [b], Știrbu Marian-Ionuț [b], Popa Ionel [c,d], Ionita Monica [a,b,e]

[a] Alfred Wegener Institute for Polar and Marine Research, Bussestr. 24, Bremerhaven 27570, Germany
[b] Forest Biometrics Laboratory – Faculty of Forestry, "Stefan cel Mare" University of Suceava, Universității Street No. 13, Suceava 720229, Romania
[c] National Research and Development Institute for Silviculture "Marin Drăcea", Calea Bucovinei 76bis, Câmpulung Moldovenesc 725100, Romania
[d] Center of Mountain Economy – INCE – CE-MONT Vatra Dornei, Petreni Street No 49, Vatra Dornei 725700, Romania
[e] Emil Racovita Institute of Speleology, Romanian Academy, Cluj-Napoca 400006, Romania

ARTICLE INFO

This manuscript was handled by Marco Borga, Editor-in-Chief

Keywords:
Streamflow reconstruction
Lower Danube
Tree rings
Oak

ABSTRACT

Paleoclimate reconstructions are increasingly used to characterize climate variability and change prior to the instrumental record, in order to improve our estimates of climate extremes and to provide a baseline for climate change projections. Most of these reconstructions are focused on temperature, precipitation, and/or drought indices and, to a lesser extent, reconstruct streamflow variability. In this study, the first regional tree-ring width chronology (i.e. *Quercus* sp.), from the Caraorman forest (Danube Delta, Romania), was used to reconstruct the last ~250 years of annual (from November previous year to July of the current year) streamflow of the Lower Danube River. The obtained results indicate a stable and significant correlation between the tree-ring width index from the Caraorman forest and the Danube streamflow at the Ceatal Izmail hydrologic station situated in the southeastern part of Europe. Interannual streamflow variation for the analyzed period indicates 14 extremely high flow years, with streamflow greater than 8780 m^3/s (1770, 1771, 1799, 1836, 1838, 1839, 1871, 1876, 1877, 1879, 1940, 1941, 1997 and 2010) and 14 extremely low flow years, with streamflow lower than 5300 m^3/s (1741, 1745, 1750, 1753, 1773, 1794, 1812, 1832, 1843, 1882, 1899, 1921, 1964 and 1994). Periods characterized by pluvials in the lower Danube Delta are associated with a low-pressure system centered over Europe, positive sea surface temperature (SST) anomalies over the Atlantic Ocean, and negative SST anomalies over the Baltic, North, and Mediterranean Seas. These large-scale conditions favor the advection of moist air from the Mediterranean and the Black Sea towards the southeastern part of Romania, which in turn leads to high precipitation rates over this region. Opposite to this, low streamflow years are associated with a high-pressure system centered over Europe, characterized by a northward shift of the storm tracks and negative SST anomalies over the Atlantic Ocean, and positive SST anomalies over the Baltic, North, and Mediterranean Seas. Based on our results, we argue that the reconstruction of river streamflow data based on the tree-ring width has important scientific and practical implications for a better understanding of the streamflow variation of the past, necessary for water resource management and environmental-hydrological protection.

1. Introduction

According to the last IPCC report (IPCC, 2022), climate change has caused substantial deterioration of ecosystems and will cause unavoidable increases in multiple climate hazards in the near and long term, causing massive damages and increasingly irreversible losses (including in terrestrial and freshwater ecosystems (IPCC, 2022). The increased frequency and intensity of climatic extremes have already led to food and water scarcity (IPCC, 2022), and represent a high risk for future water supply (Kreibich et al., 2022). In this context, planning adaptation and mitigation strategies are necessary to face the current water-related challenges and to have suitable water management. Water availability is a serious problem in densely populated and economically important regions (Boretti and Rosa, 2019; Kreibich et al., 2022), and water

* Corresponding author at: Forest Biometrics Laboratory – Faculty of Forestry, "Stefan cel Mare" University of Suceava, Universității Street No. 13, Suceava 720229, Romania.
E-mail address: nagavciuc.viorica@gmail.com (N. Viorica).

https://doi.org/10.1016/j.jhydrol.2023.129150
Received 13 September 2022; Received in revised form 29 November 2022; Accepted 20 January 2023
Available online 24 January 2023

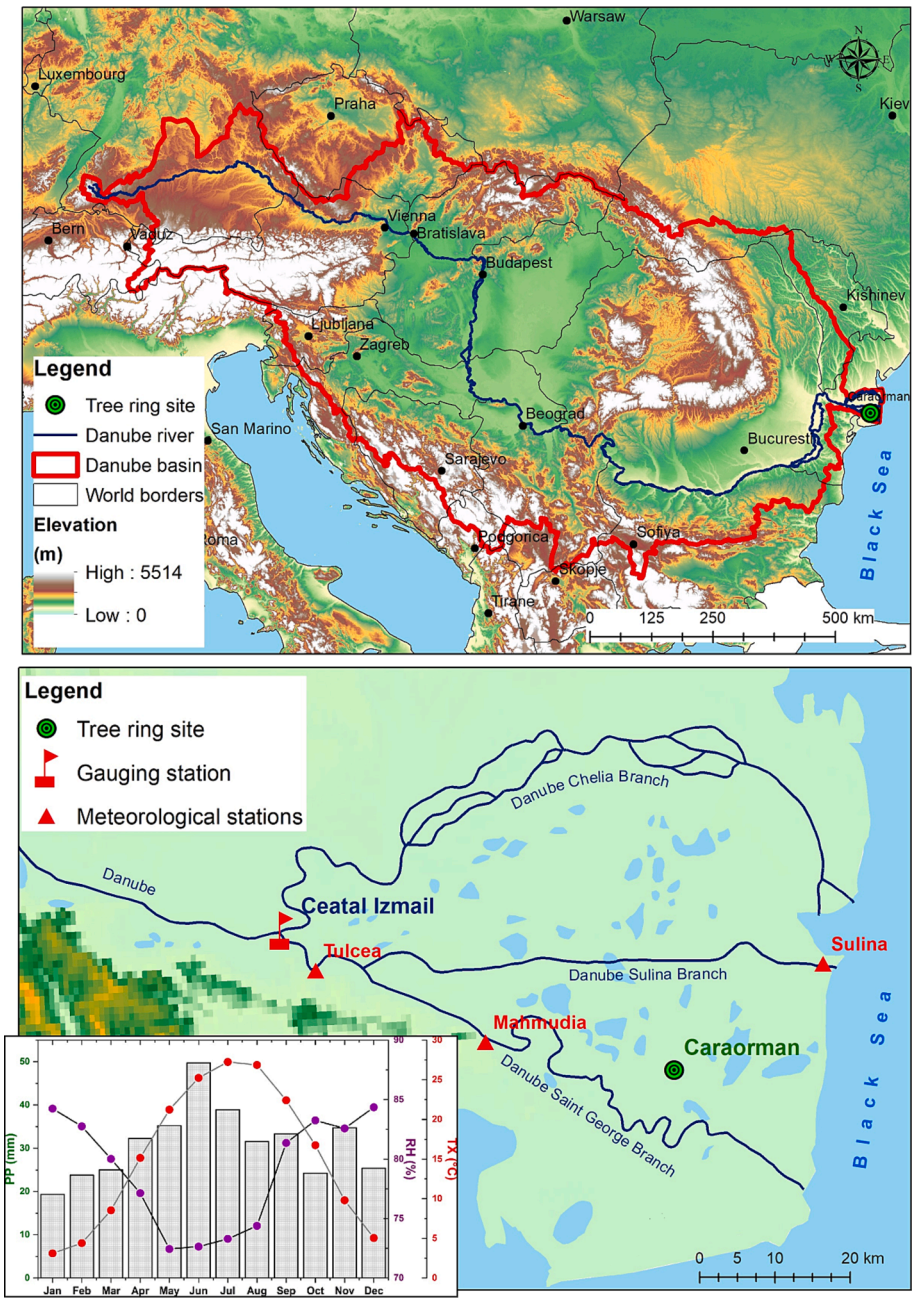

Fig. 1. Location of the investigation area in Europe (black box bottom left) and a topographic map of Romania showing the sampling site. The lower left plot represents the annual variation of the maximum temperature (red dots), precipitation (bars), and relative humidity (violet dots) over the 1961–2013 period at Mahmudia meteorological station. (For interpretation of the references to color in this figure legend, the reader is referred to the web version of this article.)

managers are increasingly confronted with supply and demand constraints on water resources, especially in Mediterranean-type climatic regions, where runoff decline is observed and expected to continue (Kundzewicz et al., 2010; Milly et al., 2005). In particular, surface runoff in the southern part of Europe, including the Danube River basin, is projected to decrease over the next few decades (Stagl and Hattermann, 2015). However, uncertainty arises from the short and, most of the time, unavailable streamflow observations.

Improvements in this respect can be facilitated by providing in-depth analyses of how hydrological extremes impact water availability and long-term climatological and hydrological information is essential to improve the accuracy of future hydrological scenarios. The development of the water resource management plan is drawn back by very short instrumental hydrological records (Van Lanen et al., 2016), which are mostly limited to 50 years (rarely reaching 100 years) for many important river basins and are not enough to capture the natural variability of hydrological variables such as streamflow. Thus, incorporating paleo, hydrological and climatological data into water management plans will help to partially solve this problem.

Tree-ring data has proven its efficiency for reconstructing different climatic parameters (e.g. precipitation and temperature), due to temporal resolution, precise dating, and its widespread availability in different parts of the globe. Tree rings are the most suitable proxies to use when it comes to building long time-scale chronologies with annual resolution. Different methodological approaches, such as tree-ring width, intra-annual density, wood anatomy or stable isotopes, are enabling us to explore the variability of multiple hydroclimatic parameters (Fritts, 1976; Gagen et al., 2004; Nagavciuc et al., 2020;

Schweingruber, 1988). However, their potential in the reconstruction of the streamflow was not fully explored. To our knowledge, there are very few published studies of streamflow reconstruction for European rivers, based on tree rings (Ballesteros-Cánovas et al., 2015; Formetta et al., 2022; Obertelli, 2020; Trlin et al., 2021), although, for regions such as the US, Canada or China, there are many more tree ring based streamflow reconstruction studies (Ballesteros-Cánovas et al., 2015; Martin et al., 2019; St. George, 2007; Wu et al., 2020; Yang et al., 2012).

In Europe, the river basin management plans are established by the European Water Framework Directive (EC, 2022). Danube river plays an essential role in the water resource availability at the European level, being the second largest river in Europe. With a catchment area of 817.000 km^2 and comprising parts of 19 countries, the river Danube sustains the life of more than 80 million people (Schiller et al., 2010). Its strategic geographical position and spatial extension are complemented by a large number of stakeholders and decision-makers who are facing significant challenges with respect to climate change and its impact on future water supply. The southern-eastern part of Romania and the Lower Danube region represent areas with high exposure to aridity, drought, and even desertification phenomenon and are especially prone to drought risks due to extreme climatic phenomena (Nagavciuc et al., 2022b). Thus, over this region, it is imperative to have long-term perspective over the current extreme hydroclimatic conditions and variability. A long-term perspective of the variability and trends of Danube River streamflow will allow different stakeholders and water managers to timely adopt the necessary precautionary measures which are needed to cushion the adverse effects of extreme events and to adapt and mitigate the current climatic conditions in order to minimize the socio-cultural impacts.

In order to provide more information on long-term streamflow variability of the Lower Danube River, which can contribute to water resource management improvement, here we report findings of the first tree-ring width based, multiseasonal streamflow reconstruction for the Lower Danube River. The overall objectives of this study are: i) to investigate the hydroclimatic sensitivity of the latewood *Quercus sp*. tree rings from Caraorman forest, Romania ii) to develop an annual (from November previous year to July current year) streamflow reconstruction for the 1734 – 2020 period for the Ceatal Izmail hydrometric station (Lower Danube) on a well-replicated tree ring dataset; iii) to investigate the long-term streamflow variability of the Lower Danube River; iv) to analyze the possible teleconnection between reconstructed streamflow data and large-scale climate patterns, and v) to describe the relative importance of the long-term river streamflow variability for water resources management.

2. Methods

2.1. Study area

Caraorman forest is located in the Danube Delta between the Sulina and Sfântu Gheorghe branches of the Danube River, in Romania (Fig. 1). Caraorman natural forest has been protected since 1938 and, from 1990 onwards it was declared a strictly protected area (2250 ha) and was included in the Danube Delta Biosphere Reserve (Administraţia Rezervaţiei Biosferei Delta Dunării, 2022). It acquired this protection status to preserve the most impressive mobile and semi-mobile dunes in the Danube Delta which can reach up to 9 m high and are partly covered with vegetation, and the Caraorman forest. Placed on a high seafront, the forest is represented by mixed oaks and other broadleaves tree species (e.g. Quercus, Fraxinus, Ulmus), with some very particular elements of species with voluble stem (e.g. *Periploca graeca*, *Vitis sylvestris*, *Humulus lupus*, *Clematis vitalba*) (Administraţia Rezervaţiei Biosferei Delta, 2022). Characterized by a temperate climate, due to its proximity to the Black Sea, the summers are usually warm and the winters are cold. The average annual temperature, at Mahmudia meteorological station (i.e., the closest meteorological station to our sampling site), is around 10.8 °C, with July as the warmest month (~22.07 °C) and January as the coldest one (~−0.39 °C). The rainfall is around 374 mm/year, with January as the driest month (~19.3 mm/month) and June as the wettest month (~50 mm/month), while the month with the highest relative humidity is December (84.35 %), and the month with the lowest relative humidity is May (72.44 %) (Fig. 1).

Table 1
A detailed list with the data sets employed in this study and their sources.

Data type	Spatial resolution	Temporal resolution	Source
Tree ring width		1728–2020	This study
Meteorological station data (precipitation, relative humidity, cloud cover, mean temperature, maximum temperature, minimum temperature)		Mahmudia: 1961–2013	Romanian National Meteorological Administration
Streamflow data		Orsova: 1921 – 2013 Tr. Magurele: 1931 – 2013 Zimnicea: 1921 – 2013 Oltenita: 1921 – 2013 Calarasi: 1931 – 2013 Braila: 1941 – 2013 Lungoci: 1935 – 2013 Ceatal Izmail: 1921 – 2013	National Institute of Hydrology and Water management Romania
Gridded precipitation data	0.5° x 0.5°	1901–2021	Harris et al., 2020
Gridded geopotential height, zonal wind and meridional winds at 500mb level	2° x 2°	1836–2015	Slivinski et al., 2021
Gridded sea surface temperature data	2° x 2°	1854–2020	Huang et al., 2018

2.2. Tree-ring chronology

During the first field trip in late autumn 2006, 36 cores (one core per tree) were collected from living dominant oak trees (*Quercus* sp.), from the Caraorman forest. In May 2021, other 42 samples (one core per tree) were collected from the same Caraorman forest, in order to update the existing sample set to the year 2020. During the second field trip, to avoid sampling the same trees, the stems were carefully checked for core marks or scars. The samples were extracted using a 5 mm Pressler increment borer following standard dendrochronological sampling methods (Schweingruber, 1988). The cores collected in 2006 were fixed in wooden supports and polished, while the cores collected in 2021 were cut using the WSL core microtome (Gärtner and Nievergelt, 2010). All samples were scanned using Silverfast v.8.1 software and an EPSON 11000 XL flatbed scanner with 1600 dpi true optical resolution and saved in a 48bit color image format. Based on the obtained images, tree-ring widths of the latewood were measured using the CooRecorder v.9.31 software (Cybis Elektronik, 2010), with a precision of 0.01 mm. All time-series were cross-dating using CDendro and checked for the missing rings using COFECHA software, using correlation analysis of 50-year intervals with a 25-year overlap (Grissino-Mayer, 2001; Holmes, 1983). We decided to use latewood for future analyses due to their demonstrated higher sensitivity to capture hydroclimatic variability (Roibu et al., 2020).

The individual raw series were transformed into a growth index

series to avoid any potential non-climatic or biological trends. All individual raw series were detrended using the negative exponential curve method in ARSTAN software (Cook and Kairiukstis, 1990). After removing the autocorrelation, the residual chronology (further described as RWI_{LW}) was used for further analyses. The temporal stability of the obtained chronology was assessed using the expressed population signal (EPS) and inter-series correlation (Rbar). EPS and Rbar were calculated using a 50-year moving window with a 25-year segment overlap (Wigley et al., 1984). The strength of the chronology signal was evaluated using a threshold value of 0.85 for the EPS parameter (Briffa and Jones, 1990).

2.3. Hydro-Climate data and statistical methods

2.3.1. Hydro-climate data

To investigate the hydroclimatic sensitivity of the latewood tree-ring width, we analyzed the correlation between RWI_{LW} and precipitation (PP), relative humidity (RH), cloud cover (CLD), mean temperature (TT), maximum temperature (TX), and minimum temperature (TN) using the data from Mahmudia meteorological station for 1961–2013 period (see location in Fig. 1). We also analyzed the relationship between RWI_{LW} and the monthly mean streamflow from seven gauging stations situated in the Lower Danube (Table 1), as well as one gauging station situated in the catchment area of Siret River (one of the main tributaries of the Danube River). In order to identify the most suitable period for paleo reconstruction, the correlation analyses start from September previous year with one month window time period until the August current year. Afterward, the time window increases with one month and the procedure is repeated. The maximum window length was 12 months. To assess the spatial stability of the correlation we used the gridded monthly precipitation (PP), covering the period 1901 – 2020, from the CRU TS v. 4.04 dataset (Harris et al., 2020).

The influence of the large-scale atmospheric circulation on the variability of high and low streamflow periods has been investigated using the monthly means of Geopotential Height at 500 mbar (mb) (Z500), zonal wind (U500), and meridional wind (V500) at 500 mb from the Twentieth Century Reanalysis (V3) data set (Compo et al., 2011, 2006; Slivinski et al., 2019) on a 2° ×2° grid, over the 1837–2015 CE period. The vertically integrated water vapor transport (WVT) (Peixoto and Oort, 1992) was calculated through zonal wind (u), meridional wind (v), and specific humidity (q), from the same data set (Compo et al., 2011; Slivinski et al., 2021). For sea surface temperature (SST), we used the Extended Reconstructed Sea Surface Temperature (ERSST) dataset V5 (spatial resolution 2° x 2°), covering the 1854 – 2020 period (Huang et al., 2018). These two large-scale datasets have been chosen for the current analysis, due to their extended length, allowing us to analyzed the large-scale drivers for ~180 years for the large-scale atmospheric circulation and ~167 years for the ocean circulation. Moreover, the same datasets have been previously used in a successful and reliable manner for paleoclimate related studies (Ionita et al., 2021; Nagavciuc et al., 2022a; Roibu et al., 2022b). A detailed list with all the dataset employed in this study is given Table 1.

2.3.2. Statistical methods

The relationship between RWI_{LW} residual chronology and the Lower Danube streamflow at the Ceatal Izmail hydrometric station was established using a linear regression model. In order to validate our model, the data was split into subsets, of approximately equal lengths, calibration (1921–1967) and verification (1968 – 2013). The explained variance (r^2), the reduction of error (RE), the coefficient of efficiency (CE), and the Durbin-Watson test (DW) statistical tests were performed to evaluate the strength and robustness of the final model. All the statistical analyses have been performed in R statistical environment, using the R packages dplR (Bunn, 2008) and treeclim (Zang and Biondi, 2015).

To test the spatial–temporal stability of the relationship between the RWI_{LW} index and climate variables (i.e. gridded monthly precipitation)

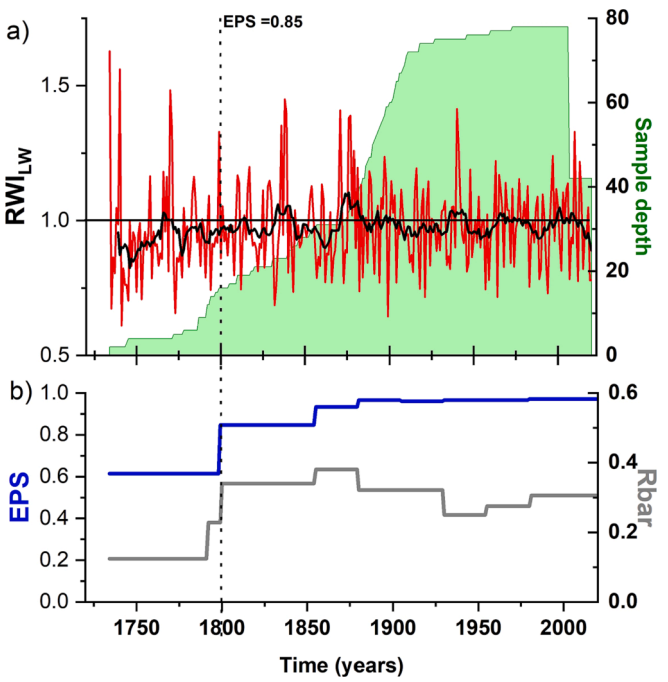

Fig. 2. Oak latewood tree-ring width chronology from Caraorman forest, Romania, and its signal strength statistics, **a)** latewood tree-ring width index (RWI_{LW}) (red line), 11-years running mean (black line), and sample replication (green outline); **b)** expressed population signal (EPS) (blue line) and inter-series correlation (Rbar) (grey line); vertical black dotted line indicates periods with EPS are greater than 0.85. (For interpretation of the references to color in this figure legend, the reader is referred to the web version of this article.)

we also make use of stability maps, a methodology successfully applied in the seasonal forecast of the European rivers and Arctic sea ice, as well as in dendroclimatological studies (Ionita et al., 2019; Ionita and Nagavciuc, 2020; Nagavciuc et al., 2020, 2019b; Roibu et al., 2022a). In order to detect stable predictors, the variability of the correlation between the RWI_{LW} time series and the monthly PP data was investigated within a 31-year moving window over the period from 1901 to 2020. The analysis was performed for a time window that starts in November of the previous year, plus one cumulative month, until June of the current year, as for this period were obtained the higher correlation coefficients. The correlation is considered stable for those regions where the RWI_{LW} index and the gridded PP data are significantly correlated at the 90 % for more than 80 % of the moving window. The advantage of this methodology, when compared with traditional correlation analysis, is the possibility to identify just the regions which have a stable relationship in time with our tree rings-based proxies. The stability maps methodology is described more in detail in Ionita, (2017).

The relationship between the large-scale oceanic (SST) and atmospheric circulation (Z500) and the reconstructed streamflow variability has been identified based on the composite maps methodology (von Storch and Zwiers, 1999). The composite maps between reconstructed streamflow and the Z500 and SST were constructed by selecting the years in which the value of the streamflow time series was higher than the 90th percentile (High) and lower than the 10th percentile (Low), respectively. This threshold was chosen as a compromise between the strength of the climate anomalies associated with streamflow anomalies and the number of maps that satisfy this criterion. Composite analysis is widely used to understand physical mechanisms and develop statistical prediction models (von Storch and Zwiers, 1999). The significance of the composite maps is based on a standard *t*-test (confidence level 95 %).

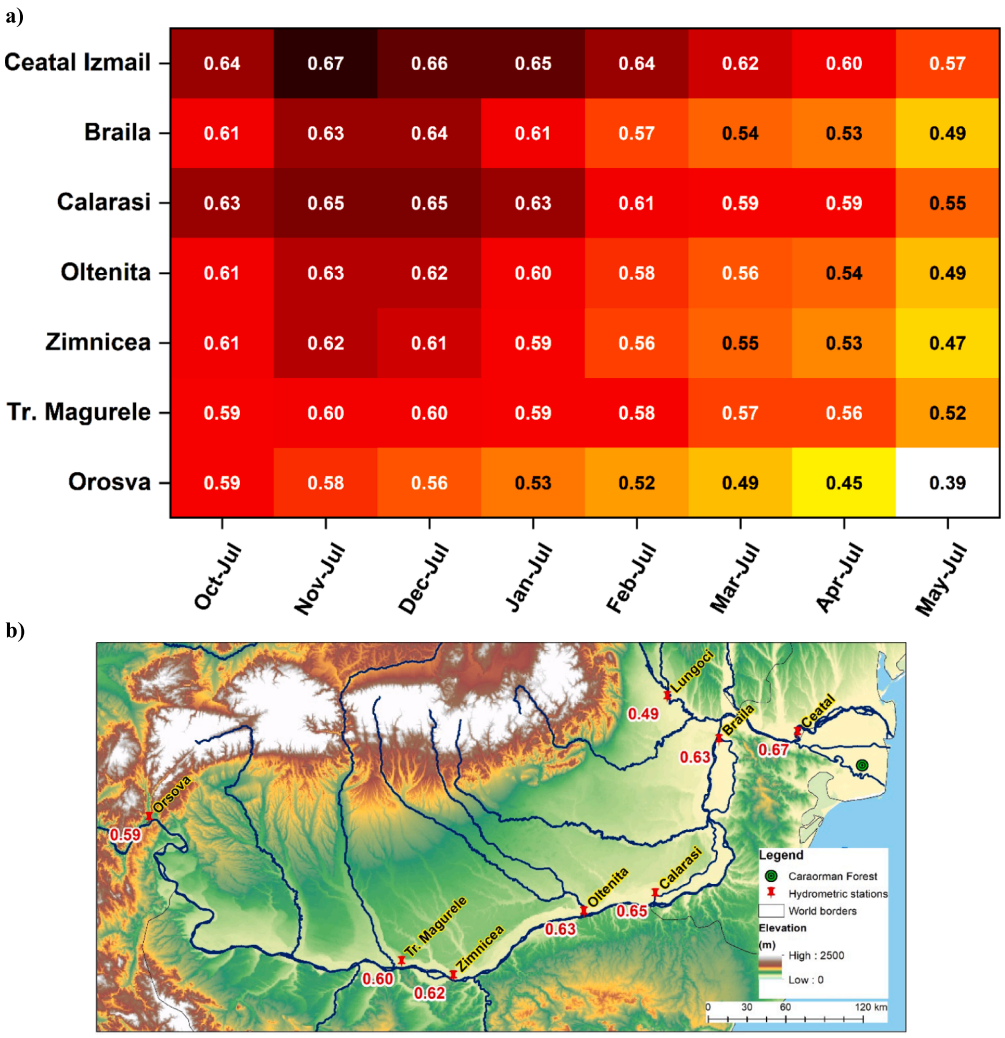

Fig. 3. A) the correlation coefficients between the RWI_{LW} index and the monthly streamflow at different gauging stations in the Lower Danube with different time lags: Oct – July (October previous year – July current year); Nov – July (November previous year – July current year), Dec – July (December previous year – July current year); Jan – July (January current year – July current year), up to May – July (May current year – July current year) and b) The spatial extent over the Lower Danube of the correlation between the RWI_{LW} index and streamflow at different gauging station for the highest correlation coefficients as identified in a). In a) all the correlation coefficients are statically significant at 95 % significance level ($p < 0.05$).

3. Results and discussion

3.1. Chronology characteristics

Here we present a new tree-ring latewood width chronology for Danube Delta, from *Quercus* sp. over the period 1728 – 2020. The length of measured cores for this study ranged between 102 and 286 annual rings, while the mean tree age is 150 years (Fig. 2). The mean tree-ring latewood width is 2.12 ± 1.26 mm. The inter-series correlation values of the individual time series range from r = 0.25 to r = 0.75 and shows a strong similarity of growth trends among the records, while the first-order autocorrelation for raw data (AC1) is 0.66. The sample replication for the last 200 years is higher than 40 series, reaching up to 78 series between 1973 and 2006. Before 1800, the sample replication decreases to 15 series. For the obtained RW_{LW} chronology, the EPS exceeds the 0.85 threshold after the year 1800 with a replication of 16 samples, which is widely accepted (Wigley et al., 1984).

3.2. RWI_{LW} hydro-climatic signal

The strength of the hydro-climate signal was evaluated by computing the monthly and seasonal (different combinations of months, from 2 to 12 months) Pearson's correlations from September of the previous year to August of the current year, between the RWI_{LW} index and different climatic parameters from Mahmudia meteorological station, as well as the monthly streamflow in the Lower Danube measured at seven gauging stations (Fig. 3, Table 2). The oak RWI_{LW} index from the Caraorman forest is negatively and significantly correlated with the maximum temperature of January (r = -0.37), March (r = −0.40), and April (r = −0.44), as well as with the January – July period (r = −0.43) (Table 2). Similar results were found for the mean temperature, but also a significant positive correlation with the previous November mean temperature (r = 0.33). For the minimum temperature, a significant and positive correlation was found only for the previous year November (r = 0.39). The RWI_{LW} index is also positive and significantly correlated with cloud cover, relative humidity, and precipitation, with the highest correlation for November previous year to July current year period (r = 0.55 for CLD, r = 0.40 for RH, and r = 0.70 for PP) (Table 2).

In terms of the streamflow correlation analyses, we found a positive and significant correlation between the RWI_{LW} index and the streamflow data through the whole Lower Danube. The highest correlation coefficient (r = 0.70, $p < 0.001$) was obtained for the Ceatal Izmail gauging station, for the case when we average the streamflow over a nine months period, namely from November previous year to July current year (Fig. 3). In the case of the other analyzed gauging stations, to correlation was the highest also for a nine-month average, namely from November previous year to July current year, except for the Orsova gauging station (Fig. 3a). For the Orsova gauging station, which is the furthest station relative to our sampling site, the highest correlations have been found for an average over 10 months (October previous year – July current year). It is noteworthy to mention that the link between streamflow variability and tree growth is defined by a complex interplay of

Table 2
Correlation coefficients of RWI_{LW} index with local monthly climate data measured at Mahmudia meteorological station and monthly streamflow data measured at Ceatal Izmail gauging station: precipitation (PP), relative humidity (RH), Cloud cover (CLD), mean temperature (TT), maximum temperature (TX), minimum temperature (TN) and streamflow (DUN). Analyzed period: 1961–2013. Correlations coefficients at 95 % significance level ($p < 0.05$) are bolded, red color indicates positive correlation and blue color indicates negative correlation.

	PP	RH	CLD	TT	TX	TN	DUN
Sep	0.22	-0.06	0.27	-0.09	-0.13	-0.06	0.16
Oct	0.15	0.11	0.26	0.09	-0.03	0.17	0.23
Nov	**0.30**	**0.38**	**0.35**	**0.33**	0.22	**0.39**	**0.29**
Dec	**0.29**	**0.32**	**0.32**	-0.07	-0.13	-0.03	**0.38**
JAN	0.22	**0.35**	**0.47**	**-0.31**	**-0.37**	-0.25	**0.38**
FEB	**0.39**	**0.40**	0.18	-0.11	-0.18	-0.06	**0.37**
MAR	0.21	0.24	**0.38**	**-0.31**	**-0.40**	-0.19	**0.53**
APR	**0.32**	0.23	0.14	**-0.32**	**-0.44**	-0.17	**0.54**
MAY	0.23	0.07	-0.14	0.06	-0.06	0.19	**0.55**
JUN	0.06	0.17	0.11	-0.08	-0.17	0.05	**0.51**
JUL	**0.29**	0.26	0.26	-0.06	-0.17	0.12	**0.44**
AUG	0.11	0.11	-0.04	0.09	0.00	0.23	**0.35**
Jan-JUL	**0.59**	**0.34**	**0.44**	**-0.30**	**-0.43**	-0.14	**0.66**
Dec-JUL	**0.62**	**0.35**	**0.47**	**-0.29**	**-0.42**	-0.13	**0.69**
Nov-JUL	**0.70**	**0.40**	**0.55**	-0.19	**-0.37**	-0.01	**0.70**

groundwater availability and climatic variability. On the one hand, tree-ring growth is influenced by a complex interaction of the temperature and precipitation (Fritts, 1976), while climatologically, the streamflow variability depends on the evapotranspiration rate which is given by water availability and temperature. Thus, the climatic factors associated with high streamflow (e.g. temperature and precipitation) are also associated with wider tree rings (Koprowski et al., 2018). On the other hand, low water availability causes a reduction in tree growth (Skiadaresis et al., 2021, 2019), furthermore, lowering the groundwater level in the area near the sea, will favor saltwater intrusion in the groundwater and soil salinization, with a negative effect on tree growth (Antonellini and Mollema, 2010; Ran et al., 2021).

The spatial–temporal stability of climatic signals was tested by applying the stability maps approach between the RWI_{LW} index and the gridded PP data over the period 1901–2020. The obtained results indicate a positive, stable, and significant correlation between our RWI_{LW} chronology and the precipitation over Ukraine, the Republic of Moldova, Romania, and Bulgaria (Fig. 4), for the cumulative period from November previous year to July current year, which represents the period for which we obtained the best spatiotemporal results. This is in agreement with the previous findings, indicating that an accumulation period of 9 months (i.e., November previous year – July current year) is the best signal for reconstructing the streamflow variability. This 9-month accumulation time can be explained also by the fact that Danube's catchment area is one of the largest in Europe and our samples location is situated close to the lowest border of it, before Danube spills into the Danube Delta, thus integrating the streamflow variability/signal throughout most of the catchment area.

Therefore, tree rings could be considered a good indicator of hydroclimatic variability because they are influenced both by groundwater availability and temperature/precipitation fluctuations, which are directly link to streamflow variability. Accordingly, a period of low streamflow (low groundwater level) determined by lack of moisture or drought conditions which represent a limiting factor for tree growth will result in narrow tree-ring width, while a period of high streamflow (high groundwater level) determined by exceeding moisture will be reflected as wide tree rings (Skiadaresis et al., 2019; Trlin et al., 2021).

3.3. Streamflow reconstruction

Taking into account all obtained correlations and the stability of the climatic signal, a linear regression model (1) was used to reconstruct the streamflow variability from the Ceatal Izmail hydrometric station averaged over the period for November previous year to July current year (Nov_{py} – Jul_{cy}) period.

$$Q_t = RWI_{LWt} * 0.48307 + 3629.15625 \quad (1)$$

where Q is streamflow for Nov_{py} – Jul_{cy} period at Ceatal Izmail hydrometric station and the RWI_{LW} is the tree-ring latewood width index of the Caraorman oak chronology at t year.

In order to evaluate the reconstruction skills, the dataset was split into two equally long periods (1922 – 1967 and 1968 – 2013) for calibration – verification approach in forward and reverse mode. The obtained highly positive values of RE and CE (Table 3), for both forward and reverse models, indicate a good and predictive reconstruction skill (Fig. 5a), while the DW values near 2 indicate little to no autocorrelation. All calibration – verification statistics suggest that the developed linear regression model is reliable for the streamflow reconstruction and can be used to reconstruct past streamflow variability. The developed reconstruction model explains 45 % ($r^2 = 0.45$) of the Danube streamflow variation at the Ceatal Izmail hydrometric station (Fig. 5b).

Based on the aforementioned linear regression model, the streamflow variability was reconstructed for the 1734 – 2020 period (Fig. 6a). Nevertheless, since the ESP value exceeded the threshold of 0.85 only after 1800, the reconstruction before 1800 might be prone to larger uncertainties. The Nov_{py} – Jul_{cy} period reconstruction of streamflow variability at the Ceatal Izmail hydrometric station preserves both the inter-annual to inter-decadal variations over the analyzed period. The interannual streamflow variability analysis revealed fourteen years with extreme low values, when the streamflow did not exceed 5300 m^3/s (<5th percentile): 1741, 1745, 1750, 1753, 1773, 1794, 1812, 1832, 1843, 1882, 1899, 1921, 1964 and 1994 and fourteen years with extreme high streamflow, over the 8780 m^3/s (>95th percentile): 1770, 1771, 1799, 1836, 1838, 1839, 1871, 1876, 1877, 1879, 1940, 1941,

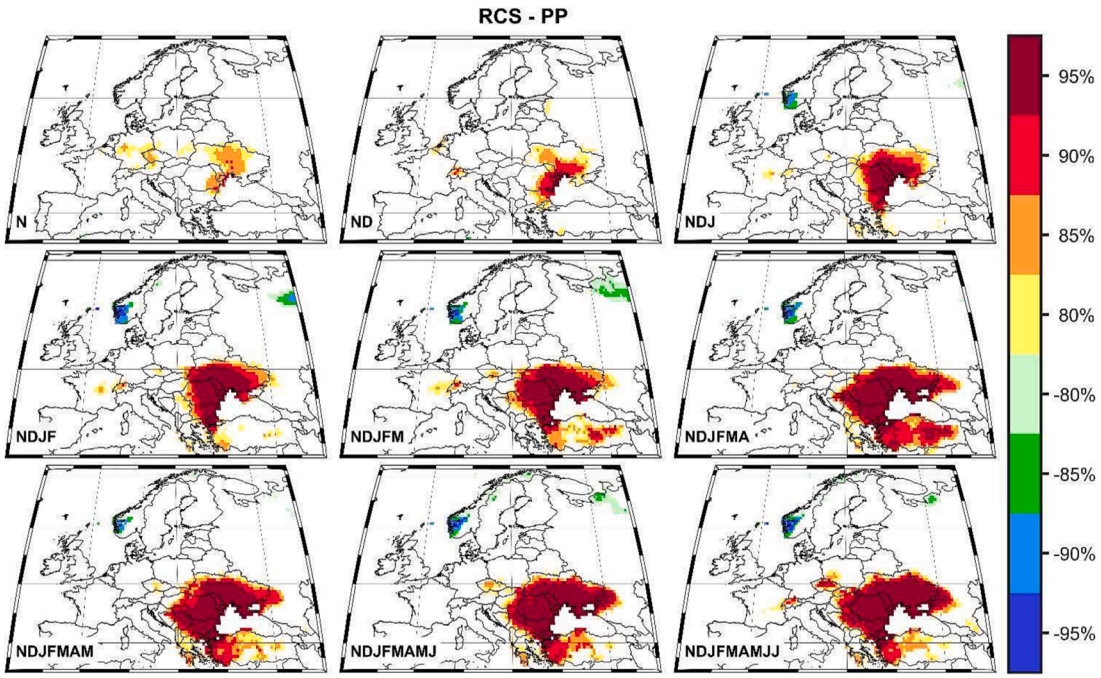

Fig. 4. Stability map of the correlation between the RWI_{LW} time series and different monthly combinations of PP from previous year November until current year July. Regions where the correlation is stable, positive, and significant for at least 80% windows are shaded with dark red (95%), red (90%), orange (85%), and yellow (80%). The corresponding regions where the correlation is stable, but negative, are shaded with a dark blue (95%), blue (90%), green (85%), and light green (80%). N—November PP from the previous year, ND – mean of November and December PP from the previous year, NDJ – mean of November and December PP from the previous year and January from the current year, NDJF – mean of November and December PP from the previous year and January and February from the current year, NDJFM – mean of November and December PP from the previous year and January, February and March from the current year, NDJFMA – mean of November and December PP from the previous year and January, February, March and April from the current year, NDJFM – mean of November and December PP from the previous year and January, February and March from the current year, NDJFMAM – mean of November and December PP from the previous year and January, February, March, April and May from the current year, NDJFM – mean of November and December PP from the previous year and January, February and March from the current year, NDJFMAMJ – mean of November and December PP from the previous year and January, February, March, April, May and June from the current year, NDJFMAMJJ – mean of November and December PP from the previous year and January, February, March, April, May, June and July from the current year. Analyzed period: 1902–2020. The significance level is computed based on a two-tailed *t*-test. (For interpretation of the references to color in this figure legend, the reader is referred to the web version of this article.)

Table 3
Summary table of calibration and verification statistics of streamflow November previous year to July current year reconstruction, Analyzed period 1921 – 2013.

Subsets lengths	r	r^2	RE	CE	DW
Early calibration (1921–1967)/late verification (1968–2013)	0.66	0.44	0.47	0.46	1.86
Early verification (1921–1967)/late calibration (1968–2013)	0.68	0.46	0.44	0.41	1.72
Full calibration period (1922–2013)	**0.67**	**0.45**			

1997 and 2010. Over the last two centuries, the periods with high streamflow occurred in the following intervals: 1830 – 1844, 1869 – 1886, 1934 – 1948, 1961–1985, and 1994 – 2014 (Fig. 6a – blue shaded areas), while periods with low streamflow occurred between 1856 and 1868, 1949 – 1960, 1986 – 1993 and from 2015 to present (Fig. 6a – red shaded areas).

To investigate the low-frequency variability of the reconstructed streamflow chronology and compare the streamflow reconstruction over different periods, we split our chronology into a 40 years window and we performed box plot statistical analyses (Fig. 6b). The median distribution of all box plots is at the same level, near 7000 m^3/s, but the distribution is different. Over the period 1821 – 1860 the majority of the streamflow data varies between 6500 and 7500 m^3/s, with the lower whisker longer than the higher ones, but with three upper outliners which indicate the presence of the extreme events. The period 1861 – 1900, is characterized by a higher variability, the first and third quartile ranging between ~6200 and 8000 m^3/s, with the longest outliners for the analyzed period. The period 1901 – 1940 is slightly skewed up, indicating that the majority of data are lower than the median. The period 1941 – 1980 is normally distributed, while the period 1981 – 2020 is characterized by a higher variability, slightly skewed up and with a much longer upper whisker than the lower one, indicating that during this period the lower Danube streamflow was predominantly lower than the median, but with some very high streamflow values.

3.4. Large-scale atmospheric circulation

Since the precipitation and temperature variability (variables that are contributing substantially to the variations of the Danube River streamflow) are mainly driven by the large-scale atmospheric circulation (Ionita, 2015; Ionita et al., 2012), we have tested also the relationship between the large-scale atmospheric circulation and our reconstructed streamflow. In order to investigate the relationship between the interannual variability of the streamflow variability and the large-scale atmospheric circulation we made use of the composite maps methodology between the streamflow reconstruction and the geopotential height at 500 mb (Z500), WVT, and SST for the cases when the streamflow was higher than the 90th percentile (>8237 m^3/s) and lower than the 10th percentile (<5545 m^3/s). The large-scale atmospheric circulation influences tree growth indirectly by influencing the intensity, duration, and variability of the climatic events. Usually, anticyclonic (cyclonic) circulation patterns determine dry (wet) climatic conditions (Ionita et al., 2015) and therefore low (high) river streamflow values, which contribute to slowing down (favors) tree growth. According to our obtained results, periods with high streamflow values are

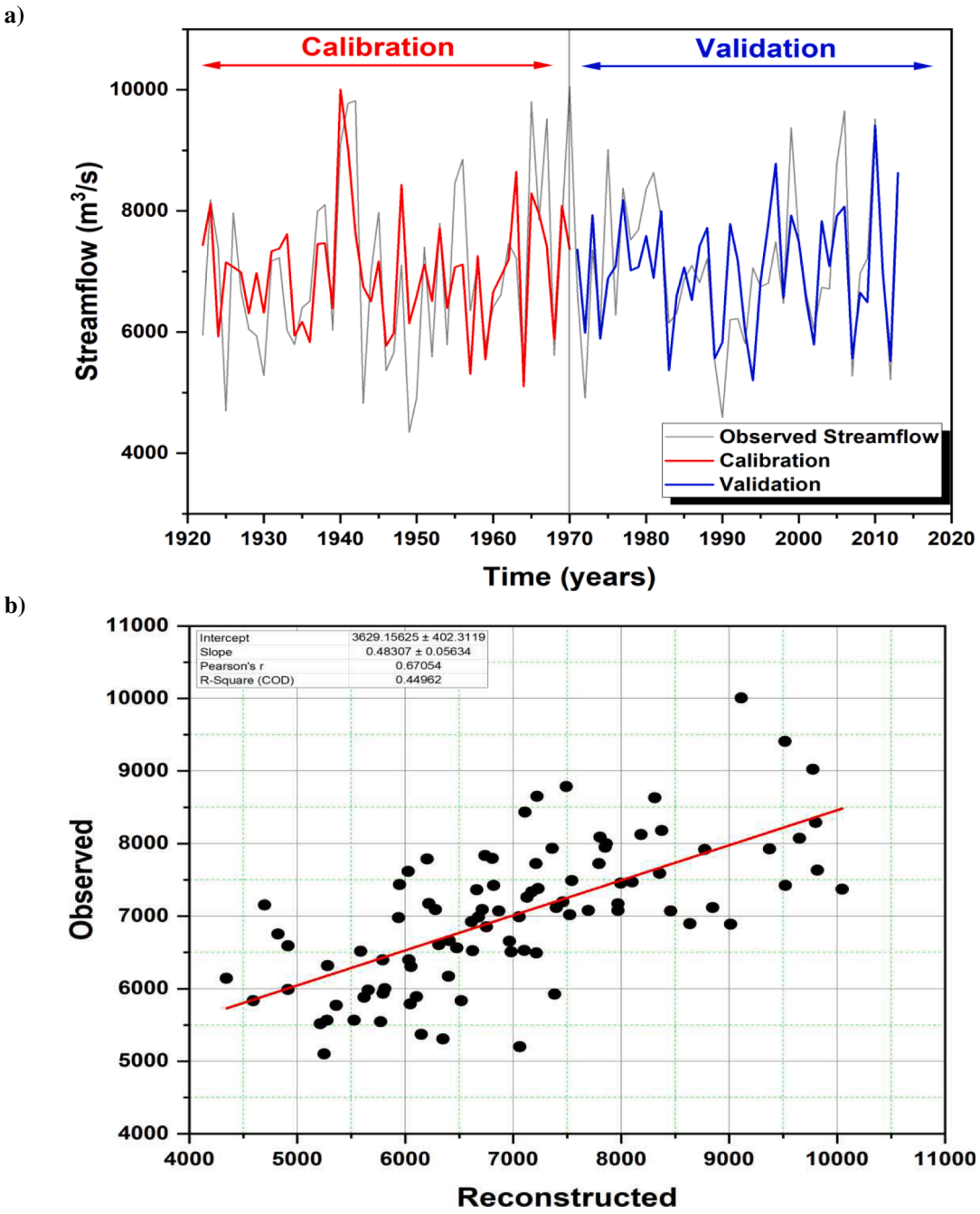

Fig. 5. A) calibration – validation model for the streamflow reconstruction. in (a) the gray line indicates the observed data; the red line indicates the reconstructed streamflow over the calibration period and the blue indicates the reconstructed streamflow over the validation period; and b) regression between the observed and reconstructed streamflow over the period 1931 – 2020. (For interpretation of the references to color in this figure legend, the reader is referred to the web version of this article.)

associated with a low-pressure system over central-western Europe and the middle Atlantic Ocean, and a high-pressure system over Greenland, Siberia, and the northern part of Africa (Fig. 7a). This pattern favors the advection of the moist air masses from the Mediterranean region toward Romania (Fig. 7c) which contributes to high precipitation rates, high streamflow, and wider tree-ring widths. Contrary to this, low flow periods are associated with a high-pressure system over central-western Europe and a low-pressure system over the northern Atlantic Ocean, Greenland, and Siberia (Fig. 7b). This pattern favors the advection of dry and warm air from the east, creating an area of local divergence over the south-eastern part of Europe (Fig. 7d), which in turn inhibits precipitation and leads to low streamflow values and narrow tree-ring widths. A similar association between the large-scale atmospheric circulation and streamflow variability over Romania, including our study region, was found by (Ionita, 2015).

The role of the Atlantic Ocean and the Mediterranean SST on the European hydroclimate variability has been highlighted by numerous previous studies (Feudale and Shukla, 2011; Ionita et al., 2017, 2012; Kingston et al., 2012). Following this line, the relationship between SST variability and tree-ring growth has been previously quantified in dendrochronological studies (Nagavciuc et al., 2020, 2019a; Roibu et al., 2022b). The analyses of the composite map reveal that the periods with high streamflow values are associated with negative SST anomalies over the seas around the Europe continent (Barents Sea, Norwegian Sea,

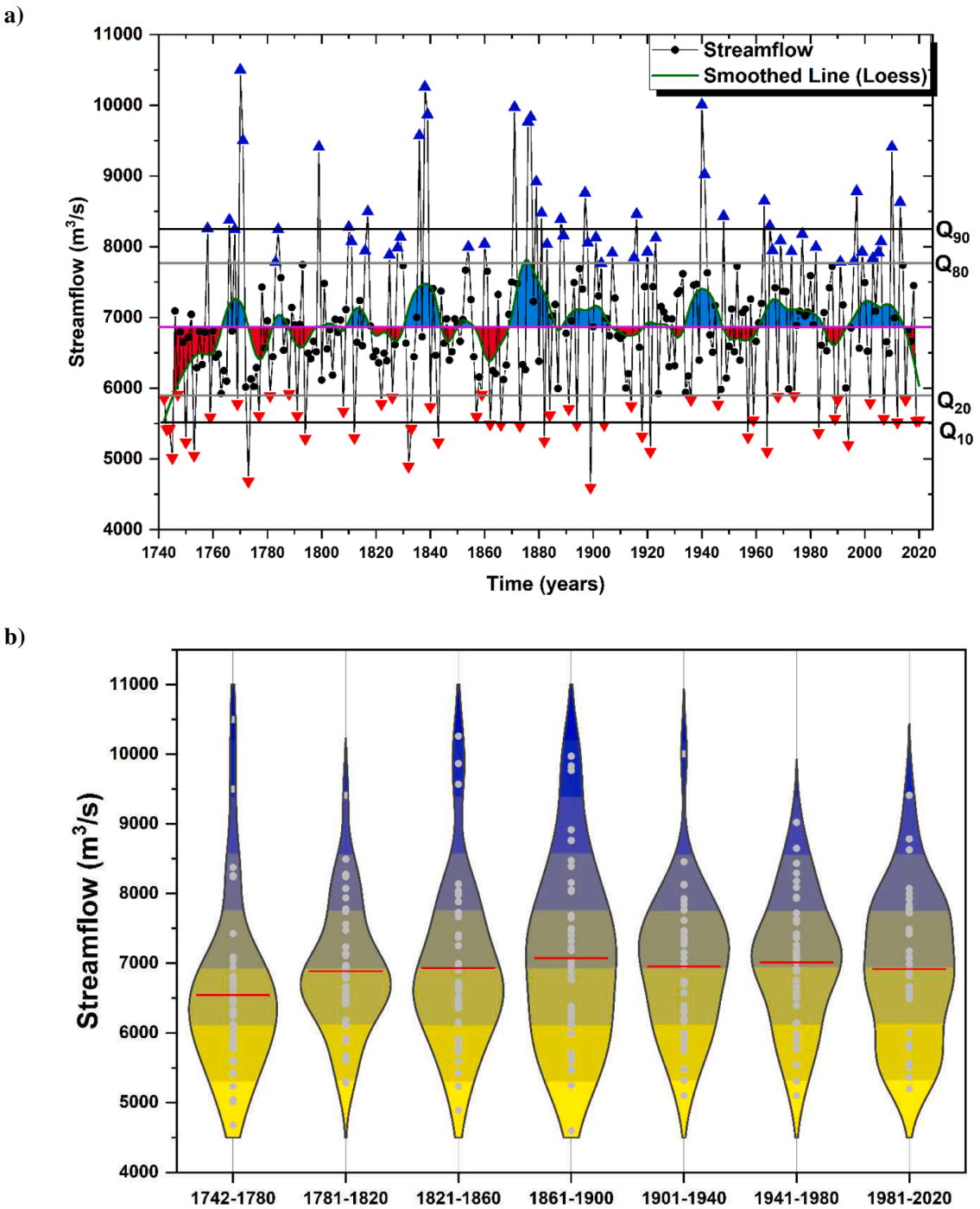

Fig. 6. The reconstructed streamflow at Ceatal Izmail for the 1728–2020 period. The green line represents a low-pass filter and the intermediate lines (grey and black) depict extreme events based on pre-defines threshold: $Q_{10,20}$ threshold (10th and 20th percentile) for low flows and $Q_{90,80}$ threshold (90th and 80th percentile) for high flows. The values above/below the grey line corresponds to the wet/dry years used in the composite map analysis (additionally marked with blue and red dots).; b) Violin plots of the reconstructed streamflow for different centuries over the period 1742 – 2020. Threshold values: Q_{10} = 5545 m^3/s, Q_{20} = 5925 m^3/s, Q_{80} = 7761 m^3/s and Q_{90} = 8237 m^3/s. (For interpretation of the references to color in this figure legend, the reader is referred to the web version of this article.)

Baltic Sea, North Sea, Celtic Sea, and the Mediterranean Sea) and positive SST anomalies over the Atlantic Ocean. Opposite to this low flow years are associated with positive SST anomalies over the seas around the Europe continent (the Barents Sea, Norwegian Sea, Baltic Sea, North Sea, Celtic Sea, and the Mediterranean Sea) and negative SST anomalies over the central and northern Atlantic Ocean (Fig. 8). The observed influence of the SST variability on the wet/dry periods in the lower Danube is in agreement with recent studies which have emphasized that the state of the Atlantic Ocean and the Mediterranean SST has a significant influence on the hydroclimate of Europe, including our analyzed region (Feudale and Shukla, 2011; Ionita et al., 2022, 2021; Kingston et al., 2015).

3.5. Implications for the River streamflow management

The Danube River streamflow is used in a variety of sectors from navigation and hydropower generation to agriculture, industry, drinking water supply, recreation, or environmental purposes (ICPDR, 2021).

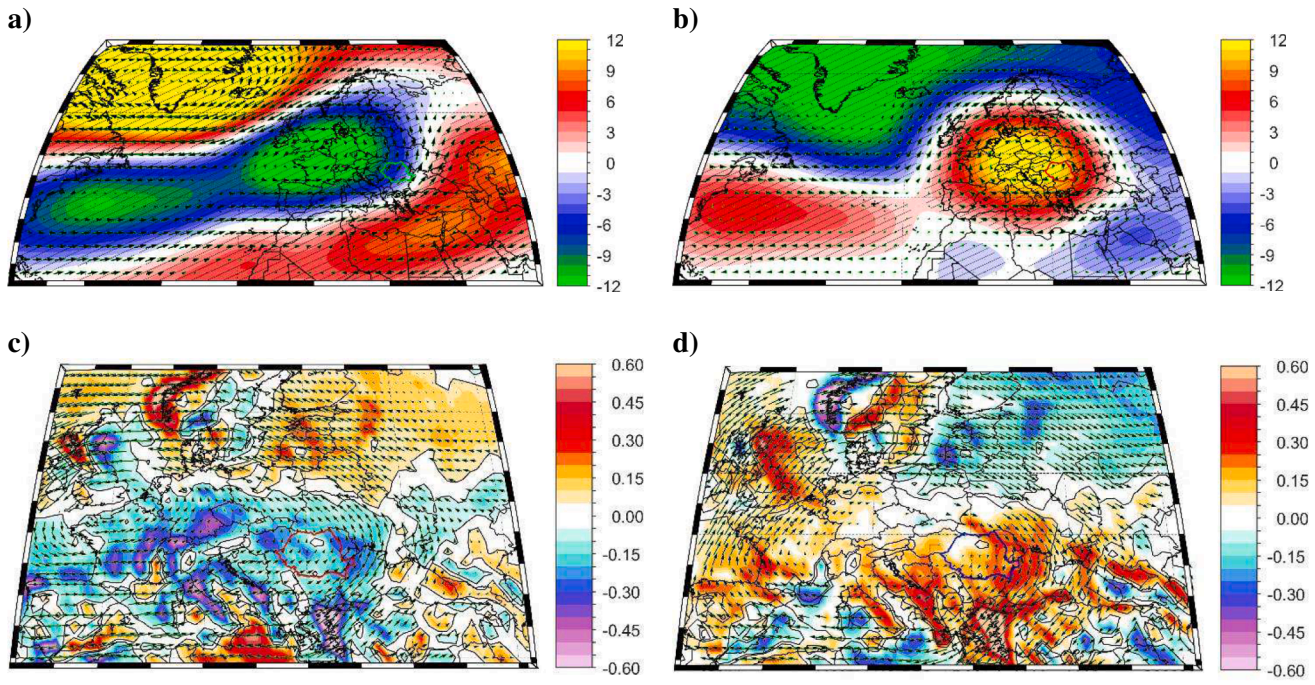

Fig. 7. a) The composite map between high streamflow years (>Q_{80}) and the mean form November previous year until July current year of the Geopotential Height at 500mb (Z500—shaded areas) and 500 mb wind vectors (arrows); b) the composite map between low streamflow years (<Q_{20}) and the mean form November previous year until July current year of the Geopotential Height at 500mb (Z500—shaded areas) and 500 mb wind vectors (arrows); c) as in a) but for the mean form November previous year until July current year of the integrated water vapor transport (WVT) and d) as in b) but for the but for the mean form November previous year until July current year of the integrated water vapor transport (WVT). The hatching in a) and b) highlights significant values at a confidence level of 95 %. Analyzed period: 1836–2015.

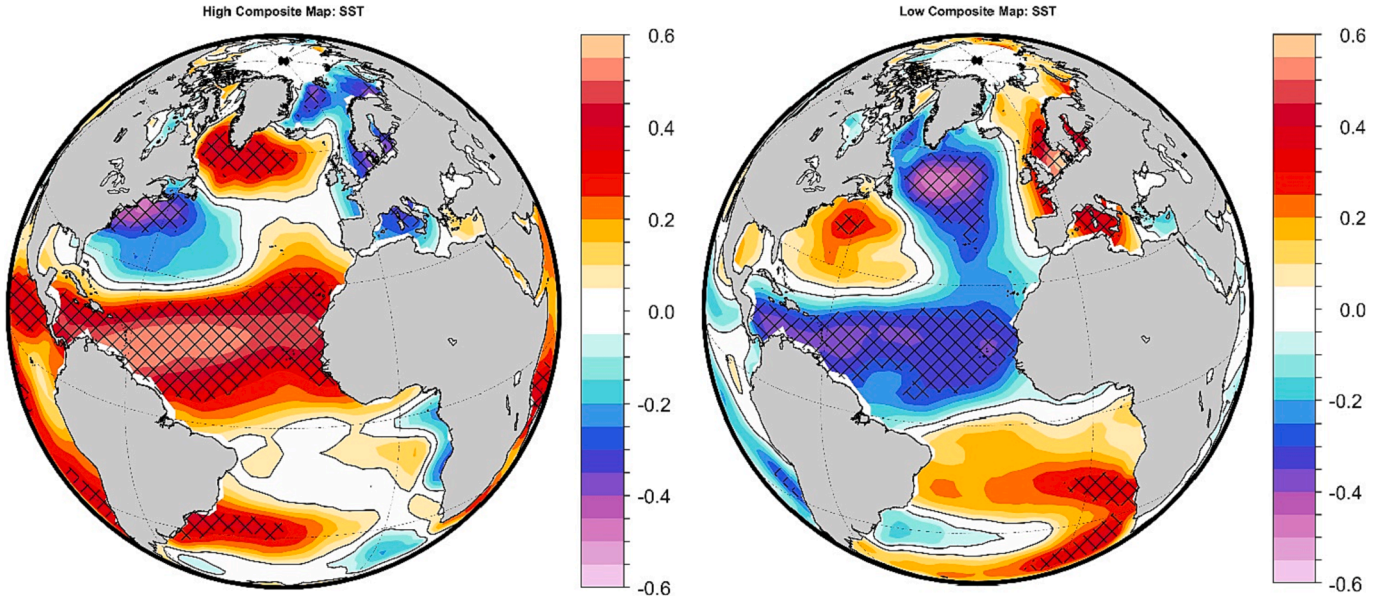

Fig. 8. a) The composite map between high streamflow years (>Q_{80}) and the mean form November previous year until July current year of the sea surface temperature (SST) and b) the composite map between low streamflow years (<Q_{20}) and the mean form November previous year until July current year of the sea surface temperature (SST). The hatching highlights significant values at a confidence level of 95 %Analyzed period: 1854 – 2020.

Therefore, streamflow variability plays a crucial role in water resource planning and management. The presented here streamflow reconstruction based on the tree-ring width is important not only for dendrohydrological studies but also for long-timescale analyses and evaluation of the Danube water availability at multi-centennial scales, especially since instrumental data are rather short (<50 years) and insufficient to capture long-scale streamflow variations, necessary for developing the hydrological models and resource water planning.

The reconstructed streamflow chronology allows us to put the instrumental record into a long-term context, indicating that the periods with the lowest (highest) streamflow from the instrumental record, are not the most extreme low (high) streamflow periods when contextualized into a longer-term perspective. For example, the low streamflow periods from the 20th century were not so extreme as the low

streamflow period from 1857 to 1870. On the flood side, the period 1871 – 1884, which was characterized by extreme high streamflow values, exceeds the streamflow rates periods from the observational periods. In addition, our reconstruction of the Lower Danube River streamflow suggests that overall, the streamflow rates were more variable at times preceding the instrumental period, implying that water management decisions are made based on relatively short and insufficient instrumental records compared with the more extensive reconstruction. Also, the streamflow from the Ceatal Izmail hydrometric station is significantly correlated with other hydrometric stations from upstream of the river (not shown) and can play a key role in decisions making and water resource management, not only at the local scale but also at the regional scale.

Considering the climate projections indicate that the impact of climate change will aggravate water availability, especially in the lower Danube basin, and will lead to a significant increase in water demand in the future (Stagl and Hattermann, 2015; Vanham, 2012), now more than ever the long-term streamflow reconstruction should be integrated into developing of the future water strategy and planning measures, to ensure feasible long term water management including industrial and human consumption water use and distribution and conservation of the features of the Danube basin.

3.6. Limitation of the study

Tree-ring width data was been proven to be an extraordinary proxy for paleoclimatic reconstruction, presenting numerous advantages over other natural proxies, nevertheless, we need to specify a few limitations. Tree-ring width, as well as all other climate proxies, contain additional noise, which add uncertainty into a chronology, however, we combined data from a very large sample of trees in order to reduce the influence of this noise. Another limitation of the study is the unavailability of instrumental climate data nearby the study site and the spatial resolution of the gridded data; however, we used the climate data from the nearest available meteorological stations (~30 km), and we used grid data sets with the best combination between spatial resolution and their extended length, thus avoiding short climatic time series which does not fulfil the study aim.

4. Conclusion

This study presents an annual streamflow reconstruction, from the Caraorman Forest (Lower Danube region), over the past ~250 years, based on the significant correlation between the tree ring latewood width and November – July streamflow ($r = 0.70$, $p < 0.001$). Our tree ring reconstruction explains ~45 % of the variance of Lower Danube streamflow, reinforcing the idea that tree rings can be also a useful proxy for streamflow (and not only for precipitation and temperature). Since our streamflow reconstruction covers only a small area, it is essential for the subsequent construction of large-scale streamflow reconstructions throughout the catchment area of the Danube River. The performance and reliability of our tree-ring based streamflow reconstruction was proved by calibration and validation of our data and by using specific statistics for the regression model over the 1931 – 2013 period. Based on our reconstruction we have identified extremely dry and wet years over the last ~250 years in the Lower Danube. Over the last ~250 years, the wettest (high streamflow) periods occurred in the following intervals: 1830 – 1844, 1869 – 1886, 1934 – 1948, 1961–1985, and 1994 – 2014. Opposite to this, the driest intervals (low flow periods) occurred between 1856–1868, 1949 – 1960, 1986 – 1993, and from 2015 to present. In general, high flow years are associated with a cyclonic circulation over the central and eastern part of Europe, convergence over the Black Sea and at country level, and positive (negative) SST anomalies in the tropical Atlantic Ocean and south of Greenland (Mediterranean Sea and North Sea). These large-scale atmospheric and oceanic anomalies lead to high precipitation rates and high streamflow in the Lower Danube. Low flow years are associated with significant divergence over the Black Sea and our analyzed region, a high-pressure system over the central part of Europe, and a cold (warm) tropical and central North Atlantic (Mediterranean Sea), which in turn inhibit precipitation.

From a water management perspective, we believe that this reconstruction can help water managers and stakeholders to improve their knowledge about the variability of the Danube streamflow, especially since streamflow observations for the Lower Danube are rather short (~50 years) or are not freely available. It is important to mention that this is the first streamflow reconstruction for the Lower Danube, helping us to put the current water issues over this region into a longer-term context. Overall, tree-rings based streamflow reconstruction enables us to better understand the long-term streamflow changes and possible trends, which could be of high value to water managers and regional planners, leading to improved support useful in the decision-making process and regional planning.

Declaration of Competing Interest

The authors declare that they have no known competing financial interests or personal relationships that could have appeared to influence the work reported in this paper.

Data availability

Data will be made available on request.

Acknowledgments

Viorica Nagavciuc was supported by a grant of the Ministry of Research, Innovation and Digitization, CNCS/CCCDI – UEFISCDI, project number PN-III-P1–1.1-PD-2019–0469, within PNCDI III. Cătălin-Constantin Roibu, Andrei Mursa and Marian-Ionuț Știrbu were supported by a grant of the Ministry of Research, Innovation and Digitization, CNCS - UEFISCDI, project number PN-III-P1-1.1-TE-2021-1419, within PNCDI III. Monica Ionita was supported by Helmholtz Association through the joint program "Changing Earth – Sustaining our Future" (PoF IV) program of the AWI. Ionel Popa was supported by a grant of the Ministry of Research, Innovation and Digitization, CNCS/CCCDI – UEFISCDI, project number PN-III-P4-PCE-2021-1002, within PNCDI III.

References

Administrația Rezervației Biosferei Delta Dunării, 2022. Conservarea Pădurii Caraorman [WWW Document]. brandware.ro.

Antonellini, M., Mollema, P.N., 2010. Impact of groundwater salinity on vegetation species richness in the coastal pine forests and wetlands of Ravenna. Italy. Ecol. Eng. 36, 1201–1211. https://doi.org/10.1016/j.ecoleng.2009.12.007.

Ballesteros-Cánovas, J.A., Stoffel, M., St George, S., Hirschboeck, K., 2015. A review of flood records from tree rings. Prog. Phys. Geogr. 39, 794–816. https://doi.org/10.1177/0309133315608758.

Boretti, A., Rosa, L., 2019. Reassessing the projections of the World Water Development Report. npj Clean Water 2, 15. https://doi.org/10.1038/s41545-019-0039-9.

Briffa, K., Jones, P.B., 1990. Basic chronology statistics and assessment. In: Cook, E.R., Kairiukstis, L. (Eds.), Methods of Dendrochronology: Applications in the Environmental Sciences. Kluwer Academic Publishers, Dordrecht, pp. 137–152.

Bunn, A.G., 2008. A dendrochronology program library in R (dplR). Dendrochronologia 26, 115–124. https://doi.org/10.1016/j.dendro.2008.01.002.

Compo, G.P., Whitaker, J.S., Sardeshmukh, P.D., 2006. Feasibility of a 100-year reanalysis using only surface pressure data. Bull. Am. Meteorol. Soc. 87, 175–190. https://doi.org/10.1175/BAMS-87-2-175.

Compo, G.P., Whitaker, J.S., Sardeshmukh, P.D., Matsui, N., Allan, R.J., Yin, X., Gleason, B.E., Vose, R.S., Rutledge, G., Bessemoulin, P., Brönnimann, S., Brunet, M., Crouthamel, R.I., Grant, A.N., Groisman, P.Y., Jones, P.D., Kruk, M.C., Kruger, A.C., Marshall, G.J., Maugeri, M., Mok, H.Y., Nordli, Ø., Ross, T.F., Trigo, R.M., Wang, X. L., Woodruff, S.D., Worley, S.J., 2011. The twentieth century reanalysis project. Q. J. R. Meteorol. Soc. 137, 1–28. https://doi.org/10.1002/qj.776.

Cook, E.R., Kairiukstis, L.A., 1990. Methods of dendrochronology. Applications in the enviromnental science, Dordrecht: Kluwer Academic Publishers; 1990. Kluwer. https://doi.org/10.1007/978-94-015-7879-0.

Cybis Elektronik, 2010. CDendro and CooRecorder. 2010. Available online: http://www.cybis.se/forfun/dendro/ index.htm. [WWW Document]. www.cybis.se.

EC, 2022. The EU Water Framework Directive – Integrated River Basin Management for Europe [WWW Document]. Eur Commision.
Feudale, L., Shukla, J., 2011. Influence of sea surface temperature on the European heat wave of 2003 summer. Part II: a modeling study. Clim. Dyn. 36, 1705–1715. https://doi.org/10.1007/s00382-010-0789-z.
Formetta, G., Tootle, G., Bertoldi, G., 2022. Streamflow reconstructions using tree-ring based Paleo Proxies for the Upper Adige River Basin (Italy). Hydrology 9. https://doi.org/10.3390/hydrology9010008.
Fritts, H.C., 1976. Tree Rings and Climate. Academic Press, London.
Gagen, M., Mccarroll, D., Edouard, J., 2004. Latewood width, maximum density, and stable carbon isotope ratios of pine as climate indicators in a dry subalpine environment. French Alps. Arctic Antarct. Alp. Res. 36, 166–171. https://doi.org/10.1657/1523-0430(2004)036[0166:LWMDAS]2.0.CO;2.
Gärtner, H., Nievergelt, D., 2010. The core-microtome: A new tool for surface preparation on cores and time series analysis of varying cell parameters. Dendrochronologia 28, 85–92. https://doi.org/10.1016/j.dendro.2009.09.002.
Grissino-Mayer, H.D., 2001. Evaluating crossdating accuracy: a manual and tutorial for the computer program COFECHA. Tree-Ring Res. 57, 205–221.
Harris, I., Osborn, T.J., Jones, P., Lister, D., 2020. Version 4 of the CRU TS monthly high-resolution gridded multivariate climate dataset. Sci. Data 7, 1–18. https://doi.org/10.1038/s41597-020-0453-3.
Holmes, R.L., 1983. Computer-assisted quality control in tree-ring dating and measurement. Tree Ring Bull. 43, 69–75.
Huang, B., Angel, W., Boyer, T., Cheng, L., Chepurin, G., Freeman, E., Liu, C., Zhang, H. M., 2018. Evaluating SST analyses with independent ocean profile observations. J. Clim. https://doi.org/10.1175/JCLI-D-17-0824.1.
ICPDR, 2021. Danube River Basin Management Plan (DRBMP) Update 2021 [WWW Document]. http://www.icpdr.org/.
Ionita, M., 2015. Interannual summer streamflow variability over Romania and its connection to large-scale atmospheric circulation. Int. J. Climatol. 35, 4186–4196. https://doi.org/10.1002/joc.4278.
Ionita, M., 2017. Mid range forecasting of the German Waterways streamflow based on hydrologic, atmospheric and oceanic data, Berichte zur Polar- und Meeresforschung = Reports on polar and marine research. Bremerhaven 711. https://doi.org/10.2312/BzPM_0711_2017.
Ionita, M., Lohmann, G., Rimbu, N., Chelcea, S., Dima, M., 2012. Interannual to decadal summer drought variability over Europe and its relationship to global sea surface temperature. Clim. Dyn. 38, 363–377. https://doi.org/10.1007/s00382-011-1028-y.
Ionita, M., Boroneanț, C., Chelcea, S., 2015. Seasonal modes of dryness and wetness variability over Europe and their connections with large scale atmospheric circulation and global sea surface temperature. Clim. Dyn. 45, 2803–2829. https://doi.org/10.1007/s00382-015-2508-2.
Ionita, M., Grosfeld, K., Scholz, P., Treffeisen, R., Lohmann, G., 2019. September Arctic sea ice minimum prediction – a skillful new statistical approach. Earth Syst. Dyn. 10, 189–203. https://doi.org/10.5194/esd-10-189-2019.
Ionita, M., Dima, M., Nagavciuc, V., Scholz, P., Lohmann, G., 2021. Past megadroughts in central Europe were longer, more severe and less warm than modern droughts. Commun. Earth Environ. 2, 61. https://doi.org/10.1038/s43247-021-00130-w.
Ionita, M., Nagavciuc, V., 2020. Forecasting low flow conditions months in advance through teleconnection patterns, with a special focus on summer 2018. Sci. Rep. 10, 13258. https://doi.org/10.1038/s41598-020-70060-8.
Ionita, M., Tallaksen, L.M., Kingston, D.G., Stagge, J.H., Laaha, G., Van Lanen, H.A.J., Scholz, P., Chelcea, S.M., Haslinger, K., Lanen, H.A.J.V., Chelcea, S.M., Haslinger, K., Scholz, P., Chelcea, S.M., Haslinger, K., 2017. The European 2015 drought from a climatological perspective. Hydrol. Earth Syst. Sci. 21, 1397–1419. https://doi.org/10.5194/hess-21-1397-2017.
Ionita, M., Nagavciuc, V., Scholz, P., Dima, M., 2022. Long-term drought intensification over Europe driven by the weakening trend of the Atlantic Meridional Overturning Circulation. J. Hydrol. Reg. Stud. 42, 101176 https://doi.org/10.1016/j.ejrh.2022.101176.
IPCC, 2022. Summary for Policymakers [H.-O. Pörtner, D.C. Roberts, E.S. Poloczanska, K. Mintenbeck, M. Tignor, A. Alegría, M. Craig, S. Langsdorf, S. Löschke, V. Möller, A. Okem (eds.)]. In: Climate Change 2022: Impacts, Adaptation, and Vulnerability. Contribution of, Ipcc.
Kingston, D.G., Fleig, A.K., Tallaksen, L.M., Hannah, D.M., 2012. Ocean-atmosphere forcing of summer streamflow drought in Great Britain. J. Hydrometeorol. https://doi.org/10.1175/JHM-D-11-0100.1, 121026084711009.
Kingston, D.G., Stagge, J.H., Tallaksen, L.M., Hannah, D.M., 2015. European-scale drought: understanding connections between atmospheric circulation and meteorological drought indices. J. Clim. 28, 505–516. https://doi.org/10.1175/JCLI-D-14-00001.1.
Koprowski, M., Okoński, B., Gričar, J., Puchałka, R., 2018. Streamflow as an ecological factor influencing radial growth of European ash (Fraxinus excelsior (L.)). Ecol. Indic. 85, 390–399. https://doi.org/10.1016/j.ecolind.2017.09.051.
Kreibich, H., Van Loon, A.F., Schröter, K., Ward, P.J., Mazzoleni, M., Sairam, N., Abeshu, G.W., Agafonova, S., AghaKouchak, A., Aksoy, H., Alvarez-Garreton, C., Aznar, B., Balkhi, L., Barendrecht, M.H., Biancamaria, S., Bos-Burgering, L., Bradley, C., Budiyono, Y., Buytaert, W., Capewell, L., Carlson, H., Cavus, Y., Couasnon, A., Coxon, G., Daliakopoulos, I., de Ruiter, M.C., Delus, C., Erfurt, M., Esposito, G., François, D., Frappart, F., Freer, J., Frolova, N., Gain, A.K., Grillakis, M., Grima, J.O., Guzmán, D.A., Huning, L.S., Ionita, M., Kharlamov, M., Khoi, D.N., Kieboom, N., Kireeva, M., Koutroulis, A., Lavado-Casimiro, W., Li, H.-Y., LLasat, M.C., Macdonald, D., Mård, J., Mathew-Richards, H., McKenzie, A., Mejia, A., Mendiondo, E.M., Mens, M., Mobini, S., Mohor, G.S., Nagavciuc, V., Ngo-Duc, T., Thao Nguyen Huynh, T., Nhi, P.T.T., Petrucci, O., Nguyen, H.Q., Quintana-Seguí, P., Razavi, S., Ridolfi, E., Riegel, J., Sadik, M.S., Savelli, E., Sazonov, A., Sharma, S., Sörensen, J., Arguello Souza, F.A., Stahl, K., Steinhausen, M., Stoelzle, M., Szalińska, W., Tang, Q., Tian, F., Tokarczyk, T., Tovar, C., Tran, T.V.T., Van Huijgevoort, M.H.J., van Vliet, M.T.H., Vorogushyn, S., Wagener, T., Wang, Y., Wendt, D.E., Wickham, E., Yang, L., Zambrano-Bigiarini, M., Blöschl, G., Di Baldassarre, G., 2022. The challenge of unprecedented floods and droughts in risk management. Nature 608, 80–86. https://doi.org/10.1038/s41586-022-04917-5.
Kundzewicz, Z.W., Lugeri, N., Dankers, R., Hirabayashi, Y., Döll, P., Pińskwar, I., Dysarz, T., Hochrainer, S., Matczak, P., 2010. Assessing river flood risk and adaptation in Europe—review of projections for the future. Mitig. Adapt. Strateg. Glob. Chang. 15, 641–656. https://doi.org/10.1007/s11027-010-9213-6.
Martin, J.T., Pederson, G.T., Woodhouse, C.A., Cook, E.R., McCabe, G.J., Wise, E.K., Erger, P., Dolan, L., McGuire, M., Gangopadhyay, S., Chase, K., Littell, J.S., Gray, S. T., George, S.S., Friedman, J., Sauchyn, D., Jacques, J.S., King, J., 2019. 1200 years of Upper Missouri River streamflow reconstructed from tree rings. Quat. Sci. Rev. 224, 105971 https://doi.org/10.1016/j.quascirev.2019.105971.
Milly, P.C.D., Dunne, K.A., Vecchia, A.V., 2005. Global pattern of trends in streamflow and water availability in a changing climate. Nature 438, 347–350. https://doi.org/10.1038/nature04312.
Nagavciuc, V., Ionita, M., Perşoiu, A., Popa, I., Loader, N.J.N.J., McCarroll, D., 2019a. Stable oxygen isotopes in Romanian oak tree rings record summer droughts and associated large-scale circulation patterns over Europe. Clim. Dyn. 52, 6557–6568. https://doi.org/10.1007/s00382-018-4530-7.
Nagavciuc, V., Roibu, C.-C.-C.-C.-C., Ionita, M., Mursa, A., Cotos, M.-G.-M.-G., Popa, I., 2019b. Different climate response of three tree ring proxies of Pinus sylvestris from the Eastern Carpathians, Romania. Dendrochronologia 54, 56–63. https://doi.org/10.1016/j.dendro.2019.02.007.
Nagavciuc, V., Kern, Z., Ionita, M., Hartl, C., Konter, O., Esper, J., Popa, I., 2020. Climate signals in carbon and oxygen isotope ratios of Pinus cembra tree-ring cellulose from Călimani Mountains. Romania. Int. J. Climatol. 40, 2539–2556. https://doi.org/10.1002/joc.6349.
Nagavciuc, V., Ionita, M., Kern, Z., McCarroll, D., Popa, I., 2022a. A ~700 years perspective on the 21st century drying in the eastern part of Europe based on δ18O in tree ring cellulose. Commun. Earth Environ. 3, 277. https://doi.org/10.1038/s43247-022-00605-4.
Nagavciuc, V., Scholz, P., Ionita, M., 2022b. Hotspots for warm and dry summers in Romania. Nat. Hazards Earth Syst. Sci. 22, 1347–1369. https://doi.org/10.5194/nhess-22-1347-2022.
Obertelli, M., 2020. A data - driven approach to streamflow reconstruction using dendrochronological data [WWW Document]. Politec. Milano 1863.
Peixoto, J.P., Oort, A.H., 1992. Physics of climate, Springer. Springer Berlin Heidelberg. https://doi.org/10.1016/0308-521X(96)86772-2.
Ran, X., Wang, X., Gao, X., Liang, H., Liu, B., Huang, X., 2021. Effects of salt stress on the photosynthetic physiology and mineral ion absorption and distribution in white willow (Salix alba L.). PLoS One 16, 1–21. https://doi.org/10.1371/journal.pone.0260086.
Roibu, C.-C., Sfecla, V., Andrei, M., Ionita, M., Viorica, N., Chiriloaei, F., Lesan, I., Ionel, P., 2020. The climatic response of tree ring width components of ash (Fraxinus excelsiorL.) and Common Oak (Quercus roburL.) from Eastern Europe. Forests 11, 600. https://doi.org/10.3390/f11050600.
Roibu, C.-C., Nagavciuc, V., Ionita, M., Popa, I., Horodnic, S.-A., Mursa, A., Büntgen, U., 2022. A tree ring-based hydroclimate reconstruction for eastern Europe reveals large-scale teleconnection patterns. Clim. Dyn. https://doi.org/10.1007/S00382-022-06255-8.
Schiller, H., Miklós, D., Sass, J., 2010. The Danube River and its Basin Physical Characteristics, Water Regime and Water Balance BT - Hydrological Processes of the Danube River Basin: Perspectives from the Danubian Countries, in: Brilly, M. (Ed.),. Springer Netherlands, Dordrecht, pp. 25–77. https://doi.org/10.1007/978-90-481-3423-6_2.
Schweingruber, F.H., 1988. Tree Rings Basics and Applications of Dendrochronology. Kluwer Academic Publishers, 10.1007/978-94-009-1273-1.
Skiadaresis, G., Schwarz, J.A., Bauhus, J., 2019. Groundwater extraction in floodplain forests reduces radial growth and increases summer drought sensitivity of Pedunculate Oak Trees (Quercus robur L.). Front. For. Glob. Chang. 2, 1–16. https://doi.org/10.3389/ffgc.2019.00005.
Skiadaresis, G., Schwarz, J., Stahl, K., Bauhus, J., 2021. Groundwater extraction reduces tree vitality, growth and xylem hydraulic capacity in Quercus robur during and after drought events. Sci. Rep. 11, 5149. https://doi.org/10.1038/s41598-021-84322-6.
Slivinski, L.C., Compo, G.P., Whitaker, J.S., Sardeshmukh, P.D., Giese, B.S., McColl, C., Allan, R., Yin, X., Vose, R., Titchner, H., Kennedy, J., Spencer, L.J., Ashcroft, L., Brönnimann, S., Brunet, M., Camuffo, D., Cornes, R., Cram, T.A., Crouthamel, R., Domínguez-Castro, F., Freeman, J.E., Gergis, J., Hawkins, E., Jones, P.D., Jourdain, S., Kaplan, A., Kubota, H., Blancq, F.L., Lee, T.-C., Lorrey, A., Luterbacher, J., Maugeri, M., Mock, C.J., Moore, G.W.K., Przybylak, R., Pudmenzky, C., Reason, C., Slonosky, V.C., Smith, C.A., Tinz, B., Trewin, B., Valente, M.A., Wang, X.L., Wilkinson, C., Wood, K., Wyszyński, P., 2019. Towards a more reliable historical reanalysis: improvements for version 3 of the Twentieth Century Reanalysis system. Q. J. R. Meteorol. Soc. 145, 2876–2908. https://doi.org/10.1002/qj.3598.
Slivinski, L.C., Compo, G.P., Sardeshmukh, P.D., Whitaker, J.S., McColl, C., Allan, R.J., Brohan, P., Yin, X., Smith, C.A., Spencer, L.J., Vose, R.S., Rohrer, M., Conroy, R.P., Schuster, D.C., Kennedy, J.J., Ashcroft, L., Brönnimann, S., Brunet, M., Camuffo, D., Cornes, R., Cram, T.A., Domínguez-Castro, F., Freeman, J.E., Gergis, J., Hawkins, E., Jones, P.D., Kubota, H., Lee, T.C., Lorrey, A.M., Luterbacher, J., Mock, C.J., Przybylak, R.K., Pudmenzky, C., Slonosky, V.C., Tinz, B., Trewin, B., Wang, X.L., Wilkinson, C., Wood, K., Wyszynski, P., 2021. An evaluation of the performance of

the twentieth century reanalysis version 3. J. Clim. 34, 1417–1438. https://doi.org/10.1175/JCLI-D-20-0505.1.

St. George, S., 2007. Streamflow in the Winnipeg River basin, Canada: trends, extremes and climate linkages. J. Hydrol. 332, 396–411. https://doi.org/10.1016/j.jhydrol.2006.07.014.

Stagl, J.C., Hattermann, F.F., 2015. Impacts of climate change on the hydrological regime of the danube river and its tributaries using an ensemble of climate scenarios. Water (Switzerland) 7, 6139–6172. https://doi.org/10.3390/w7116139.

Trlin, D., Mikac, S., Žmegač, A., Orešković, M., 2021. Dendrohydrological reconstructions based on tree-ring width (Trw) chronologies of narrow-leaved ash in the sava river basin (croatia). Sustain. 13, 1–11. https://doi.org/10.3390/su13042408.

Van Lanen, H.A.J.H.A.J., Laaha, G., Kingston, D.G.D.G., Gauster, T., Ionita, M., Vidal, J.-P.-J.-P., Vlnas, R., Tallaksen, L.M.L.M., Stahl, K., Hannaford, J., Delus, C., Fendekova, M., Mediero, L., Prudhomme, C., Rets, E., Romanowicz, R.J.R.J., Gailliez, S., Wong, W.K.W.K., Adler, M.-J.-M.-J., Blauhut, V., Caillouet, L., Chelcea, S., Frolova, N., Gudmundsson, L., Hanel, M., Haslinger, K., Kireeva, M., Osuch, M., Sauquet, E., Stagge, J.H.J.H., Van Loon, A.F.A.F., 2016. Hydrology needed to manage droughts: the 2015 European case. Hydrol. Process. 30, 3097–3104. https://doi.org/10.1002/hyp.10838.

Vanham, D., 2012. The Alps under climate change: Implications for water management in Europe. J. Water Clim. Chang. 3, 197–206. https://doi.org/10.2166/wcc.2012.032.

von Storch, H., Zwiers, F.W., 1999. Statistical Analysis in Climate Research, Statistical Analysis in Climate Research. Cambridge University Press. https://doi.org/10.1017/cbo9780511612336.

Wigley, T.M.L., Briffa, K.R., Jones, P.D., 1984. On the average value of correlated time series, with applications in dendroclimatology and hydrometeorology. J. Clim. Appl. Meteorol. 23, 201–213.

Wu, Y., Gan, T.Y., She, Y., Xu, C., Yan, H., 2020. Five centuries of reconstructed streamflow in Athabasca River Basin, Canada: Non-stationarity and teleconnection to climate patterns. Sci. Total Environ. 746 https://doi.org/10.1016/j.scitotenv.2020.141330.

Yang, B., Qin, C., Shi, F., Sonechkin, D.M., 2012. Tree ring-based annual streamflow reconstruction for the Heihe River in arid northwestern China from ad 575 and its implications for water resource management. Holocene 22, 773–784. https://doi.org/10.1177/0959683611430411.

Zang, C., Biondi, F., 2015. Treeclim: an R package for the numerical calibration of proxy-climate relationships. Ecography (Cop.) 38, 431–436. https://doi.org/10.1111/ecog.01335.